

JGR Atmospheres

RESEARCH ARTICLE

10.1029/2018JD029976

Key Points:

- $\text{NH}_4^+/\text{NH}_3$ and pH had a more nonlinear relationship during highly polluted periods, compared to less polluted periods
- $\text{NH}_4^+/\text{NH}_3$ (g) was important for stabilizing pH during the heavily polluted periods
- SOR was higher than NOR under conditions with high acidity, light pollution, and low water content in the winter

Supporting Information:

- Supporting Information S1
- Data Set S1

Correspondence to:

Y. Feng and A. G. Russell,
fengyc@nankai.edu.cn;
ted.russell@gatech.edu

Citation:

Shi, G., Xu, J., Shi, X., Liu, B., Bi, X., Xiao, Z., et al. (2019). Aerosol pH dynamics during haze periods in an urban environment in China: Use of detailed, hourly, speciated observations to study the role of ammonia availability and secondary aerosol formation and urban environment. *Journal of Geophysical Research: Atmospheres*, 124, 9730–9742. <https://doi.org/10.1029/2018JD029976>

Received 13 NOV 2018

Accepted 17 JUN 2019

Accepted article online 8 JUL 2019

Published online 20 AUG 2019

Author Contributions:

Conceptualization: Guoliang Shi

Data curation: Guoliang Shi, Jiao Xu, Xiaohui Bi, Kui Chen, Jie Wen, Yingze Tian

Formal analysis: Baoshuang Liu, Xiaohui Bi, Jie Wen, Shihao Dong

Investigation: Baoshuang Liu, Xiaohui Bi, Kui Chen, Jie Wen, Shihao Dong, Yingze Tian

Methodology: Guoliang Shi, Jiao Xu, Xurong Shi

Resources: Kui Chen, Shihao Dong, Yingze Tian

Software: Jiao Xu, Jie Gao

Writing - original draft: Guoliang Shi, Jiao Xu, Xurong Shi
(continued)

©2019. American Geophysical Union.
All Rights Reserved.

Aerosol pH Dynamics During Haze Periods in an Urban Environment in China: Use of Detailed, Hourly, Speciated Observations to Study the Role of Ammonia Availability and Secondary Aerosol Formation and Urban Environment

Guoliang Shi¹, Jiao Xu¹, Xurong Shi¹, Baoshuang Liu¹, Xiaohui Bi¹, Zhimei Xiao², Kui Chen², Jie Wen¹, Shihao Dong¹, Yingze Tian¹, Yinchang Feng¹, Haofei Yu³ , Shaojie Song⁴, Qianyu Zhao¹, Jie Gao¹, and Armistead G. Russell⁵ 

¹State Environmental Protection Key Laboratory of Urban Ambient Air Particulate Matter Pollution Prevention and Control, College of Environmental Science and Engineering, Nankai University, Tianjin, P.R. China, ²Tianjin Eco-Environmental Monitoring Center, Tianjin, P.R. China, ³Department of Civil, Environmental and Construction Engineering, University of Central Florida, Orlando, FL, USA, ⁴School of Engineering and Applied Sciences, Harvard University, Cambridge, MA, USA, ⁵School of Civil and Environmental Engineering, Georgia Institute of Technology, Atlanta, GA, USA

Abstract Aerosol pH is a useful diagnostic of aerosol chemistry for formation of secondary aerosol and has been hypothesized to be a key factor in specific chemical reaction routes producing sulfate and nitrate. In this study, we measured hourly concentrations of water-soluble ions in particulate matter with an aerodynamic diameter less than 2.5 μm , along with gaseous pollutants in Tianjin, China, from 4 to 31 January 2015. The following source contributions to water-soluble ions were estimated by positive matrix factorization: secondary sulfate (13%), secondary nitrate (44%), coal (14%), vehicle (16%), and dust (13%). ISORROPIA-II was used to investigate the complex relationships among aerosol pH, ammonia, and secondary aerosol formation. The estimated hourly aerosol pH varied from -0.3 to 7.7 , with an average of 4.9 (± 0.78); the median value was 4.89 , and the interquartile range was 0.72 . During less polluted conditions, aerosol pH ranged from less than 0 to about 7 ; during heavily polluted conditions, pH was close to 5 (3.9 – 7.9) despite large amounts of sulfate. Sufficient ammonia/ammonium was present to balance high sulfate and nitrate formation. $\text{NH}_4^+/\text{NH}_3$ (g) helped stabilize pH while nonvolatile cations contributed less to decreasing aerosol acidity. High acidity ($\text{pH} < 3$), light pollution (total water soluble ions $< 30 \mu\text{g}/\text{m}^3$), and low water content (less than $5 \mu\text{g}/\text{m}^3$) were more correlated with higher rates of sulfate formation than nitrate formation in the winter.

Plain Language Summary Megacities in China and elsewhere experience very smoggy days that get continuously worse during haze episodes. The high levels of smog are created both from directly emitted particles and the formation of more particulate matter from gas-phase reactions. Scientists are not able to fully explain how so much smog is formed so rapidly during intense haze periods. Ammonia was found to stabilize the acidity of the aerosols, but the aerosols remained acidic with pH of around 4. Here detailed hourly measurements of many species are used to elucidate the importance of ammonia, which can potentially neutralize acidic gases and aqueous particles.

1. Introduction

Aerosol acidity, as characterized by pH (hydrogen ion activity expressed on a logarithmic scale), influences aerosol growth and concentrations via secondary aerosol formation and gas-aerosol partitioning (Jang et al., 2002; H. Y. Li et al., 2018; Meskhidze et al., 2003; Pattatytus et al., 2018; Surratta et al., 2010). Fine particulate matter, much of which can be acidic (Lawal et al., 2018; Silvern et al., 2017; Song et al., 2018, 2019; Weber et al., 2016), is also associated with harmful effects on human health. Particulate matter can also have negative environmental effects, such as reduced visibility and damage to ecological systems and historical monuments (Bouwman et al., 2002; Cheng et al., 2011; Huo et al., 2012; Ren et al., 2011; Tang et al., 2010; W. Wang, Liu, et al., 2006). A particular focus is on fine aerosols, that is, $\text{PM}_{2.5}$ (particulate matter with an

Writing – review & editing: Guoliang Shi, Haofei Yu, Shaojie Song, Qianyu Zhao, Jie Gao

aerodynamic diameter less than 2.5 μm) because of the associated health and visibility impacts, along with the associated regulatory issues.

Previous studies have found that aerosol pH varies spatially and temporally in response to secondary aerosol formation, meteorological conditions, and primary emissions of water-soluble (WS) ions and gaseous precursors (Hu et al., 2014; Yue et al., 2009; Zhang et al., 2012). Inorganic WS ions including NH_4^+ , SO_4^{2-} , and NO_3^- generally account for one third of particulate matter mass in urban atmospheres (Liu et al., 2008; Putaud et al., 2004; Yang et al., 2011) and are major determinants of aerosol pH (Cheng et al., 2011; He et al., 2012). Emissions of NH_3 (g) gas lead to the formation of NH_4^+ , which plays an important role in neutralizing acidic aerosol particles (McMurry et al., 1983; Murphy et al., 2017) and reacts with HNO_3 (g) and other acidic gases to form secondary aerosol. In addition, highly hygroscopic inorganic species like NH_4^+ , SO_4^{2-} , and NO_3^- are closely associated with aerosol water content, which affects aerosol pH (Guo et al., 2015; L. J. Li et al., 2018; Murphy et al., 2017).

Systematic studies that link aerosol pH with primary source emissions and secondary formation mechanisms and identify the primary drivers of spatiotemporal pH variations are still scarce despite the important role pH may play (Shi et al., 2017). Specifically, the effect of the availability and behavior of NH_3 (g) and NH_4^+ on aerosol pH is still poorly understood. In this study, we used ISORROPIA-II (Fountoukis & Nenes, 2007; Guo et al., 2015; Song et al., 2018), a gas-aerosol thermodynamics equilibrium model and detailed hourly field observations to investigate the relationships among aerosol pH, sources of emissions of WS ions and their precursors (especially NH_3 (g) and NH_4^+), and secondary formation of inorganic aerosols. ISORROPIA-II has been applied in many past studies and has proven to be effective in calculating aerosol water content and pH (Guo et al., 2015; Shi et al., 2017).

2. Methods and Materials

2.1. Sampling Sites and Chemical Analysis

2.1.1. Sampling Sites

Sampling was conducted in the center of Tianjin, a coastal megacity in the North China Plain, from 4 to 31 January 2015 (Figure S1). Samples were collected 22 m above ground level in an area surrounded by residential buildings and located approximately 200 m away from a heavily trafficked major road. As found by others (Gao et al., 2015; Shao et al., 2018; Yu et al., 2019), fine particulate is the dominant mode for PM in winter. In Shen et al.'s (2011) work, $\text{PM}_{2.5}/\text{PM}_{10}$ ratios were about 0.71; while the ratios of NH_4^+ , NO_3^- , and SO_4^{2-} for $\text{PM}_{2.5}/\text{PM}_{10}$ were 0.98, 0.85, and 0.89 in winter. In Shao et al.'s (2018) work, $\text{PM}_{2.5}/\text{PM}_{10}$ ratios were 0.82–0.86, and ratios of NH_4^+ , NO_3^- , and SO_4^{2-} for $\text{PM}_{2.5}/\text{PM}_{10}$ were 0.93, 0.97, and 0.80 during haze episodes. In Yu et al.'s (2019) work, the $\text{PM}_{2.5}/\text{PM}_{10}$ ratio was 0.80 and ratio of ion subtotal (NH_4^+ , NO_3^- , and SO_4^{2-}) for $\text{PM}_{2.5}/\text{PM}_{10}$ was 0.83 in winter. In Shen et al.'s (2009) work, the $\text{PM}_{2.5}/\text{TSP}$ ratio was about 0.52 during haze episodes, and the ratios of NH_4^+ , NO_3^- , and SO_4^{2-} for $\text{PM}_{2.5}/\text{TSP}$ were 0.96, 0.80, and 0.84. In Q. Zhang et al.'s (2015) work, the $\text{PM}_{2.5}/\text{TSP}$ ratio was about 0.54 during haze episodes in winter, while the ratios of NH_4^+ , NO_3^- , SO_4^{2-} , Na^+ , K^+ , and Cl^- for $\text{PM}_{2.5}/\text{TSP}$ were 0.8, 0.8, 0.7, 0.7, 0.8, and 0.7. Some base cations (such as Ca^{2+} and Mg^{2+}) showed relatively lower ratios (0.3 and 0.4) for $\text{PM}_{2.5}/\text{TSP}$; however, their concentrations were lower (10.8 and 0.7 $\mu\text{g}/\text{m}^3$ for Ca^{2+} and Mg^{2+}) than those of NH_4^+ (23.6 $\mu\text{g}/\text{m}^3$), NO_3^- (36.6 $\mu\text{g}/\text{m}^3$), and SO_4^{2-} (55.3 $\mu\text{g}/\text{m}^3$; Q. Zhang et al., 2015). Based on the findings of previous studies and due to the concern with its impacts about health impacts and haze, this work focuses on fine mode particulate.

2.2. Aerosol Water-Soluble Ion Analysis

Inorganic WS ions were measured hourly by an ambient ion monitor (AIM, URG Corporation, URG9000B). The AIM instrument was operated with a denuder to capture gases (such as HNO_3 gas) that would otherwise interfere with the aerosol measurements. The same instrument has been successfully used in several field campaigns (Shi et al., 2017; Wu & Wang, 2007). Briefly, the instrument consists of a particle collection unit and two ion chromatographs (IC) for chemical analysis. The sample inlet was equipped with a $\text{PM}_{2.5}$ sharp-cut cyclone and the samples were collected at a flow rate of 3 L/min.

The URG9000B has the capability to measure mass concentrations of major inorganic ions in aerosols using two ICs, including five major cations (NH_4^+ , Na^+ , K^+ , Ca^{2+} , Mg^{2+}), five anions (SO_4^{2-} , NO_3^- , Cl^- , F^- ,

NO₂⁻) and gases (such as HNO₃ gas, etc). The analysis is performed using 20 mM methanesulfonic acid for cation analysis and 0.08 mM sodium carbonate/0.01 mM sodium bicarbonate for the anion system. Both ICs are operated in isocratic elution at a flow rate of 0.5 mL/min.

Coarse mode particle composition measurements were not made during this period. Coarse mode PM can react with nitric acid gas to form coarse mode nitrate (Gao et al., 2015; Shao et al., 2018) and remove nitric acid, thus preventing it from affecting the thermodynamics of the PM_{2.5} fraction.

2.2.1. Measurements of Trace Gases

Hourly concentrations of trace gaseous pollutants (including NH₃(g), SO₂, NO₂, O₃, and CO) were measured. SO₂, NO₂, O₃, and CO were measured using commercially available instruments (Thermo Instruments, Model 42i for NO₂, Model 43i for SO₂, Model 48i for CO, Model 49i for O₃). NH₃ (g) was measured by the Thermo Scientific™ Model 17i.

2.3. Source Apportionment Modeling

Positive matrix factorization (PMF) is a useful tool to infer potential source contributions of particulate matter. In this work, PMF was used to estimate the source contributions to total water-soluble ions (TWI). PMF (Paatero & Tapper, 1994) attempts to decompose the data matrix X (m × n: m is the number of samples and n is the number of chemical species) into two matrices: the source profile matrix F (P × n: P is the number of source categories) and the source contribution matrix G (m × P). F and G are constrained to be nonnegative (Al-Dabbous & Kumar, 2015; Habre et al., 2011; Liu et al., 2008; Manousakas et al., 2015; Parworth et al., 2015):

$$x_{ij} = \sum_{p=1}^P g_{ip} f_{pj} + e_{ij} \quad (i = 1, \dots, I, j = 1, \dots, J), \quad (1)$$

where x_{ij} is the measured concentration of the j th species in the i th sample, f_{pj} is the concentration of the j th species in p th source, g_{ip} is the contribution of p th source to the i th sample, e_{ij} is the portion of the measurements that cannot be fitted by the model (residuals), and p is the number of factors (Amato et al., 2009; Amato & Hopke, 2012; Paatero & Tapper, 1994).

The goal of PMF is to minimize the “objective function” Q , which is the sum of the squares of residuals, e_{ij} , weighted inversely by the standard variation δ_{ij}^2 of the data values x_{ij} :

$$Q(E) = \sum_{i=1}^m \sum_{j=1}^n (e_{ij}/\delta_{ij})^2 ; e_{ij} = x_{ij} - \sum_{p=1}^P g_{ip} f_{pj} \quad i = 1, 2, \dots, m; j = 1, 2, \dots, n \quad (2)$$

where e_{ij} is the “residual” for the j th compound of the i th sample and σ_{ij} is the “uncertainty” in the j th compound of the i th sample, which is used to downweight corresponding observations that include sampling errors, uncertainties associated with detection limits, missing data, and outliers (Paatero, 2007). Specifically, the online ambient measurement data set (ions and gases) was introduced into the PMF model to develop a set of factors that can be linked to potential source contributions. In this work, x_{ij} is the measured concentration of the j th WS ions in the i th sample, f_{pj} is the concentration of the j th WS ions in p th source, and g_{ip} is the contribution of p th source to TWI for the i th sample. More detailed information can be found in our previous works (Shi et al., 2017) and the supporting information.

2.4. Calculation of Ion Balance of Particulate Matter

In addition to chemical composition, PM_{2.5} acidity is also important as a diagnostic of aerosol composition and effects on potential chemical reaction routes (Cheng et al., 2014; Sun et al., 2010). The ratio of AE (anion equivalents) and CE (cation equivalents) has been used to indicate the acidity of atmospheric aerosol (Gao et al., 2015). The calculation of particulate anion and cation equivalents are as follows (Gao et al., 2015):

$$AE = [\text{NO}_3^-]/62 + [\text{SO}_4^{2-}]/48 + [\text{Cl}^-]/35.5 \quad (3)$$

$$CE = [\text{NH}_4^+]/18 + [\text{Ca}^{2+}]/20 + [\text{K}^+]/39 + [\text{Mg}^{2+}]/12 + [\text{Na}^+]/23 \quad (4)$$

where $[\text{NO}_3^-]$, $[\text{SO}_4^{2-}]$, $[\text{Cl}^-]$, $[\text{NH}_4^+]$, $[\text{Ca}^{2+}]$, $[\text{K}^+]$, $[\text{Mg}^{2+}]$, and $[\text{Na}^+]$ represent the mass concentration ($\mu\text{g}/\text{m}^3$) of these ionic species in the $\text{PM}_{2.5}$ samples. The ratio of AE/CE has been used to represent the acidity of particulate matter (Gao et al., 2015). AE/CE ratios close to 1 suggest that particles are more neutral, ratios larger than 1 indicate that particles are in acidic condition, and ratios smaller than 1 indicate alkaline conditions. We have adopted this approach for the purpose of investigating ion balance. We acknowledge its limitations (Hennigan et al., 2015) and do not attempt to accurately characterize aerosol pH using this approach.

2.5. Aerosol pH Calculation

ISORROPIA-II (http://nenes.eas.gatech.edu/ISORROPIA/index_old.html or <https://isorropia.epfl.ch>) was applied in this work to calculate aerosol pH (Fountoukis & Nenes, 2007). ISORROPIA-II is a thermodynamic equilibrium model for the $\text{K}^+\text{-Ca}^{2+}\text{-Mg}^{2+}\text{-NH}_4^+\text{-Na}^+\text{-SO}_4^{2-}\text{-NO}_3^-\text{-Cl}^-\text{-H}_2\text{O}$ aerosol system (Fountoukis & Nenes, 2007; Weber et al., 2016). It has been used in many studies to estimate aerosol pH. Further descriptions of this model can be found elsewhere (Fountoukis & Nenes, 2007; Guo et al., 2015; Weber et al., 2016). In this study, ISORROPIA-II was executed in the forward mode and the metastable state. In the forward mode, total concentrations, including gas and WS-ion concentrations, are input into the model, while the reverse mode only requires WS-ion concentrations. Observed inorganic gases and condensed phase pollutant concentrations, including Na^+ , SO_4^{2-} , TNH_4^+ ($\text{NH}_4^+ + \text{NH}_3(\text{g})$), TNO_3^- ($\text{NO}_3^- + \text{HNO}_3(\text{g})$), Cl^- , Ca^{2+} , K^+ , and Mg^{2+} , along with relative humidity and temperature data, were input into ISORROPIA-II to calculate pH. Results from past studies suggest that this approach works well, and it closely reproduces observed species partitioning between gas phase and aerosol constituents (Fountoukis & Nenes, 2007; Murphy et al., 2017). Additionally, we used E-AIM (mode IV; <http://www.aim.env.uea.ac.uk/aim/model4/model4a.php>) to calculate activity coefficients and pH and to examine the effect of the activity coefficients on pH. E-AIM (mode IV) models the $\text{H}^+\text{-NH}_4^+\text{-Na}^+\text{-SO}_4^{2-}\text{-NO}_3^-\text{-Cl}^-\text{-H}_2\text{O}$ system. Crustal cations (e.g., Ca^{2+} , Mg^{2+} , and K^+) can be considered as an equivalent amount of Na^+ . Mode IV of E-AIM (mode IV) is limited to RHs above 60%.

2.6. Calculation of Secondary Formation Rates

The formation of ions is closely related to their corresponding gaseous precursors (Ziemba et al., 2007). Sulfate can originate from primary emissions, such as coal combustion, and also from secondary formation. In this work, we mainly focus on secondary sulfate, whose contributions are estimated by PMF. Thus, we refer to sulfate as “secondary sulfate” ($(\text{NH}_4)_2\text{SO}_4$) henceforth. Sulfate is formed from SO_2 through gas-phase, liquid-phase, and heterogeneous processes, although a small fraction is directly emitted as a product of combustion (Pandis & Seinfeld, 1989). Nitrate is formed from reactive oxidized nitrogen compounds and their oxidation products. Ammonium is formed from $\text{NH}_3(\text{g})$, the primary alkaline trace gas in the atmosphere, reacting with atmospheric acids such as nitric (HNO_3), hydrochloric (HCl), and sulfuric acids (H_2SO_4). In this work, we assume that nitrate and sulfate are secondary. SOR (sulfur oxidation ratio; equation (5)) and NOR (nitrogen oxidation ratio; equation (6)) are indices measuring the extent to which SO_2 and NO_2 are converted to SO_4^{2-} and NO_3^- (Colbeck & Harrison, 1984; Kaneyasu et al., 1999; Ohta & Okita, 1990; Xu et al., 2017):

$$\text{SOR} = \frac{\text{SO}_4^{2-}}{\text{SO}_4^{2-} + \text{SO}_2} \quad (5)$$

$$\text{NOR} = \frac{\text{NO}_3^- + \text{HNO}_3(\text{g})}{\text{NO}_3^- + \text{HNO}_3(\text{g}) + \text{NO}_2} \quad (6)$$

where SOR is the ratio of sulfate sulfur to “total” sulfur (as sulfate plus sulfur dioxide) and NOR is the ratio of nitrate nitrogen and $\text{HNO}_3(\text{gas})$ to “total” oxidized nitrogen (as nitrate, $\text{HNO}_3(\text{gas})$ plus nitrogen dioxide). High SOR and NOR values imply that the photochemical oxidation of precursor gases has led to the near-total conversion of gaseous precursors to sulfate- and nitrate-containing secondary aerosol. The measurements here do not provide organic sulfate or nitrate aerosols and gases.

We also calculated NOR* and SOR*, using NO_x and s- SO_4^{2-} (SO_4^{2-} estimated to come from secondary formation) in the calculation. Additional discussion is presented in the supporting information. In past work,

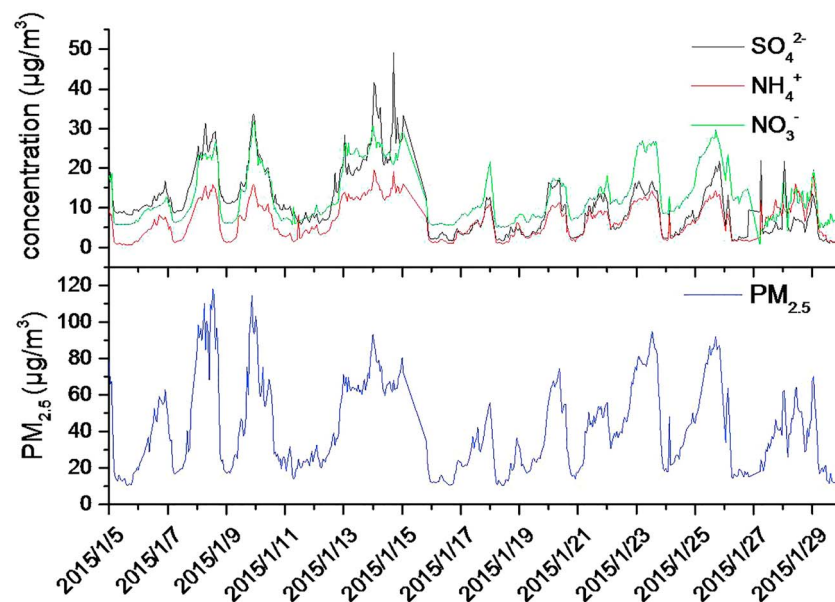


Figure 1. Temporal concentration variations of inorganic water-soluble ions and $\text{PM}_{2.5}$. For each species, hourly concentrations were observed. Good correlations among SO_4^{2-} , NO_3^- , and NH_4^+ were obtained: $R = 0.78$ for SO_4^{2-} and NO_3^- , $R = 0.80$ for SO_4^{2-} and NH_4^+ , and $R = 0.86$ for NO_3^- and NH_4^+ . Detailed information for other ions and gases are provided in Figure S3.

NO_2 and SO_4^{2-} were more frequently used for NOR and SOR, so in this work, we focus on the SOR and NOR results, noting that the use of NOR* and SOR* does not change the result of the discussion.

3. Results and Discussion

3.1. Aerosol pH

Using high temporal resolution (1-hr) online instruments, we measured concentrations of WS ions and gaseous pollutants in Tianjin (Figure S1), a megacity in China, during January 2015, a period with multiple intense haze episodes (Figures 1 and S3). It is recognized that aerosol pH can vary with particle size, and the available measurements are only for $\text{PM}_{2.5}$, without further size segregation. Also, the role of organic matter (concentrations of which were not available) has been shown to be relatively small (0.3 pH units) in other studies, and thus, it is not considered here (Fang et al., 2017; Guo et al., 2015, 2016). To evaluate the performance of ISORROPIA-II, we compared the concentrations calculated by ISORROPIA-II with measurements for NH_3 (g), NH_4^+ , NO_3^- , and HNO_3 (g). The regression plot of calculated NH_3 (g) against measured values is shown in Figure S2. For NH_3 (g), NH_4^+ , and NO_3^- slopes were from 0.66 to 0.91 with Pearson's R of 0.88–0.94. However, HNO_3 (gas) has a low and negative correlation: -0.15 . This is due, in part, to the high ammonia levels making the modeled HNO_3 (gas) more sensitive to errors in species measurements. In addition to ISORROPIA-II, we used E-AIM to calculate the pH and the H^+ activity coefficients for some samples to compare the pH estimated by different models and to evaluate the effect of the H^+ activity coefficient on pH. For the same samples, we found the mean pH from E-AIM was 4.1, a little bit lower than from ISORROPIA-II (mean pH = 4.7), and the influence of H^+ activity coefficients on pH was weaker than that of H^+ molality ($\log_{10}\gamma(\text{H}^+) = 0.32 \pm 0.22$, $\gamma(\text{H}^+)$ is the activity coefficient of H^+), which agrees well with other recent assessments (Jia et al., 2018; Song et al., 2018).

NH_4^+ , SO_4^{2-} , and NO_3^- were found to be the most abundant inorganic WS ions, contributing to approximately 70% of TWI (Figure 1). Concentrations of these WS ions increase with levels of their precursor gases (SO_2 , HNO_3 (g), and NH_3 (g); Figure S3) and with total PM levels. The estimated aerosol pH ranged from -0.3 to 7.7 , with an average value of 4.9 ± 0.8 (mean \pm SD); the median value was 4.89 and the interquartile range was 0.72. Most of the aerosol pH values were around 4–6, with only a small fraction of aerosols having a pH above 7 or below 4 based on bulk composition. We found that aerosol pH changed considerably at

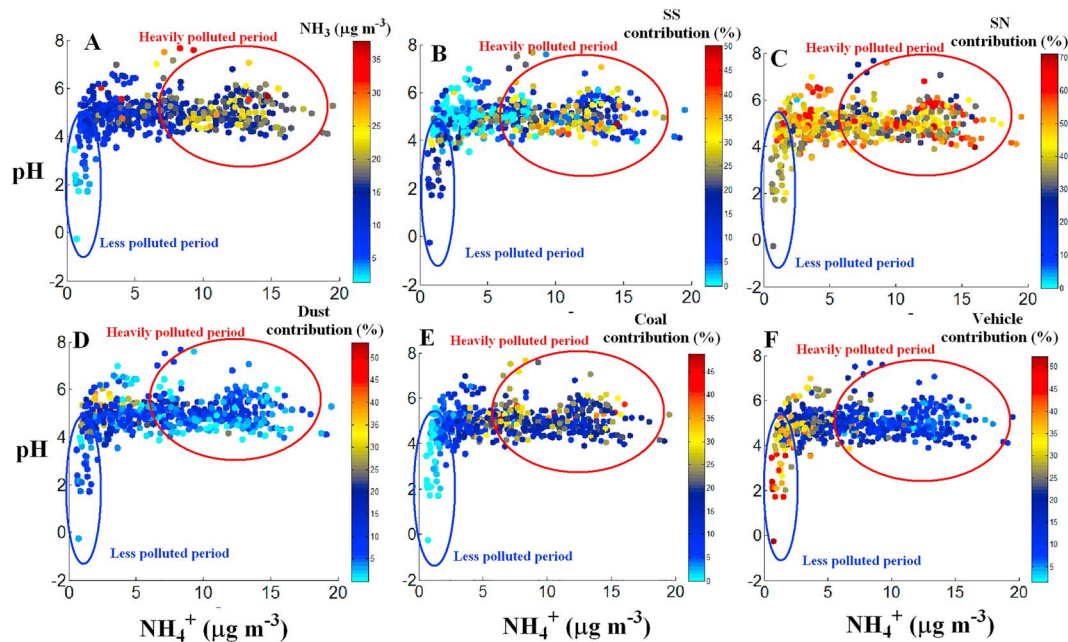


Figure 2. Relationship between pH and NH_4^+ at different source contribution levels. In less polluted time periods (blue circle), pH increases with NH_4^+ levels. In heavily polluted time periods (red circle), pH stayed in a narrow range. Heavily polluted periods were typically dominated by secondary sulfate; as sulfate increased, so did NH_4^+ . Less polluted period: total WS-ion concentrations (TWI) $< 30 \mu\text{g}/\text{m}^3$. Heavily polluted period: total WS-ion concentrations (TWI) $> 30 \mu\text{g}/\text{m}^3$. SS = secondary sulfate, SN = secondary nitrate.

different pollution levels (as characterized by TWI; Figures S4a and S6). During less polluted time periods (TWI $< 30 \mu\text{g}/\text{m}^3$), aerosol pH varied more (from -0.3 to 7.0 with an average of 4.7 ± 0.9) and was typically acidic (except for a very small fraction with pH higher than 6). During highly polluted time periods (TWI $> 30 \mu\text{g}/\text{m}^3$), aerosol pH changes were smaller (from 3.9 to 7.7 with an average of 5.0 ± 0.6). A statistically significant difference ($p < 0.01$) in pH was found between the highly polluted and less polluted time periods.

3.2. Aerosol pH and $\text{NH}_4^+/\text{NH}_3$ (g)

Similar results were observed between aerosol pH and measured NH_4^+ (and measured NH_3 (g); Figures 2 and 3). When NH_4^+ or gas-phase NH_3 (g) are found at lower levels ($\text{NH}_4^+ < 3 \mu\text{g}/\text{m}^3$), aerosol pH increases along with concentration of NH_4^+ or NH_3 (g) (see Figure 2, blue circle). During more polluted time periods (Figures 2 and 3, blue circle), aerosol pH is relatively constant as measured NH_4^+ (or NH_3 (g)) concentrations increases. At higher pollution levels, the relationship between pH and ammonia/ammonium becomes more nonlinear. Figure S8 also shows the nonlinear relationship between activity coefficients and NH_4^+ concentrations at high pollution levels. This shows that ammonia availability has a critical effect on pH when pollution levels are low, but these conditions occur in a minority of cases. Another study suggested that pH would increase by 1 unit for a factor of 10 increase in NH_3 (g) (Guo et al., 2017), which is consistent with our findings for lower concentrations but not for higher pollution levels. This is due, in part, to thermodynamic buffering and different source contributions (increased dust and coal fly ash levels) during more heavily polluted time periods and because aerosol nitrate formation becomes more thermodynamically favorable at lower temperature and moderate pH (3–6) due both to the abundance of ammonia/ammonium and nonvolatile cations.

3.3. Source Influence on pH

In order to explore source influence on pH, PMF was applied to analyze the source contribution to TWI. Five factors were resolved (Figure S5): secondary sulfate (13% of TWI), secondary nitrate (44% of TWI), coal combustion (14% of TWI), vehicle exhaust (16% of TWI), and crustal dust (including construction dust and road

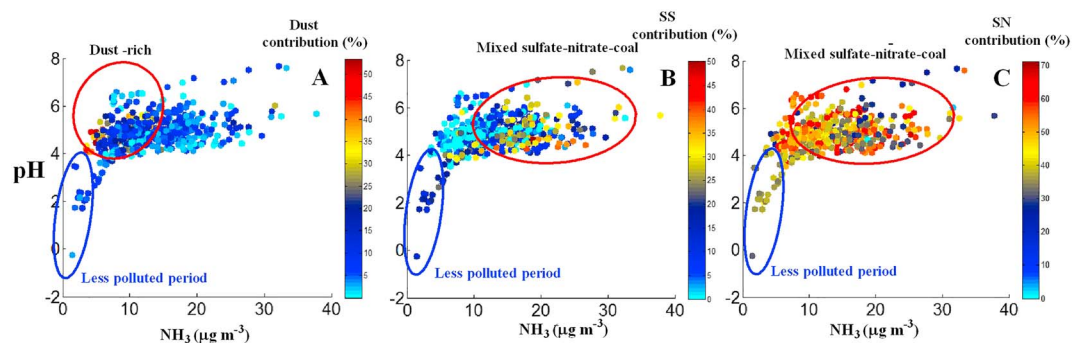


Figure 3. Relationship between NH_3 (g) and aerosol pH at different source contribution levels. pH versus NH_3 (g) and (a) dust, (b) secondary sulfate, and (c) secondary nitrate contributions.

dust; 13% of TWI). In the relationship between pH and ammonium/ammonia, periods that were dust-rich and mixed sulfate-nitrate-coal regions were identified according to the relative contributions of those factors (Figure 3). Table S1 shows the average source contribution (%), concentrations ($\mu\text{g}/\text{m}^3$) of NH_3 (g) and TWI, and pH in dust-rich and mixed regions. Dust-rich PM has a relatively high pH (4.8) and occurs at lower ammonia gas levels ($<10 \mu\text{g}/\text{m}^3$; Figure 3) due to the higher levels of dust (15%) which contributed nonvolatile cations. The mixed sulfate-nitrate-coal region typically occurs with high ammonia gas levels ($>15 \mu\text{g}/\text{m}^3$, heavily polluted period; Figure 3), and the pH range remains relatively constant (around 4–6; average of 5.1). During haze episodes, although there is more sulfate and nitrate present due to cations associated with coal combustion (i.e., both in the primary PM as well as the ammonium associated with sulfate formation), there is also ammonia available, leading to less acidic aerosol compared with typical conditions during clean periods.

Additionally, we tested the correlations between pH and source contributions ($\mu\text{g}/\text{m}^3$) under less and more heavily polluted levels and found that coal (Pearson's $R = 0.21$ during heavily polluted periods and 0.27 during less polluted periods) and dust (Pearson's $R = 0.12$ during heavily polluted periods and 0.26 during less polluted periods) showed weak positive relationships with pH while vehicles (Pearson's $R = -0.08$ during heavily polluted periods and -0.13 during less polluted periods) and secondary sulfate (Pearson's $R = -0.05$ during heavily polluted periods and -0.22 during less polluted periods) showed weak negative relationships (Table 1). This is because dust and coal contributed more cations (Ca^{2+} , Mg^{2+} , NH_4^+ , etc.) while vehicles and secondary sulfate contributed more anions (SO_4^{2-}) or NO_x (precursor of NO_3^-). However, it is notable that the correlation between pH and secondary nitrate were weakly negative (Pearson's $R = -0.05$) during heavily polluted conditions while moderately positive (Pearson's $R = 0.40$) for less polluted conditions. The low correlations show that the relationship between pH and sources is nonlinear, which is not surprising considering that pH is measured on a nonlinear (log) scale, that the activity coefficients will respond in a nonlinear fashion, and that the underlying chemistry is nonlinear. It is interesting that the absolute values of R in heavily polluted periods were lower than those during less polluted periods. This can be tied, in part, to the nonlinearities in both the activity coefficients and to the overall chemistry becoming increasingly nonlinear at high pollutant loadings. As seen in Figures 2 and 3, pH and $\text{NH}_4^+/\text{NH}_3$ have a more linear relationship during less polluted periods (blue circles) while at higher concentrations the relationship is more nonlinear (red circles).

We suspect that such differences are caused by the poor or rich NH_4^+ conditions in clean and polluted periods, and we use the concept of “excess $[\text{NH}_4^+]$ ” to explore the relationship. Here excess $[\text{NH}_4^+]$ is defined as the amount of ammonium in excess of that required for $[\text{NH}_4^+]/[\text{SO}_4^{2-}] = 1.5$ and is calculated as $[\text{NH}_4^+] - 1.5 \times [\text{SO}_4^{2-}]$ in molar concentration (Huang et al., 2011). During less polluted periods (pH 2–4), the excess $[\text{NH}_4^+]$ was less than 0, indicating a poor NH_4^+ condition. The secondary nitrate increased along with NH_4^+ (Figure 2c), leading to pH increases. During heavily polluted periods, NH_4^+ is in moderate ($0 < \text{excess}$

Table 1
Pearson's R Between Hourly Serial pH and Source Contribution, TWI ($\mu\text{g}/\text{m}^3$)

	Coal	Dust	Vehicle	SN	SS	TWI
Heavily polluted	0.21	0.12	-0.08	-0.05	-0.05	-0.02
Less polluted	0.28	0.26	-0.13	0.40	-0.23	0.11

SN = secondary nitrate, SS = secondary sulfate.

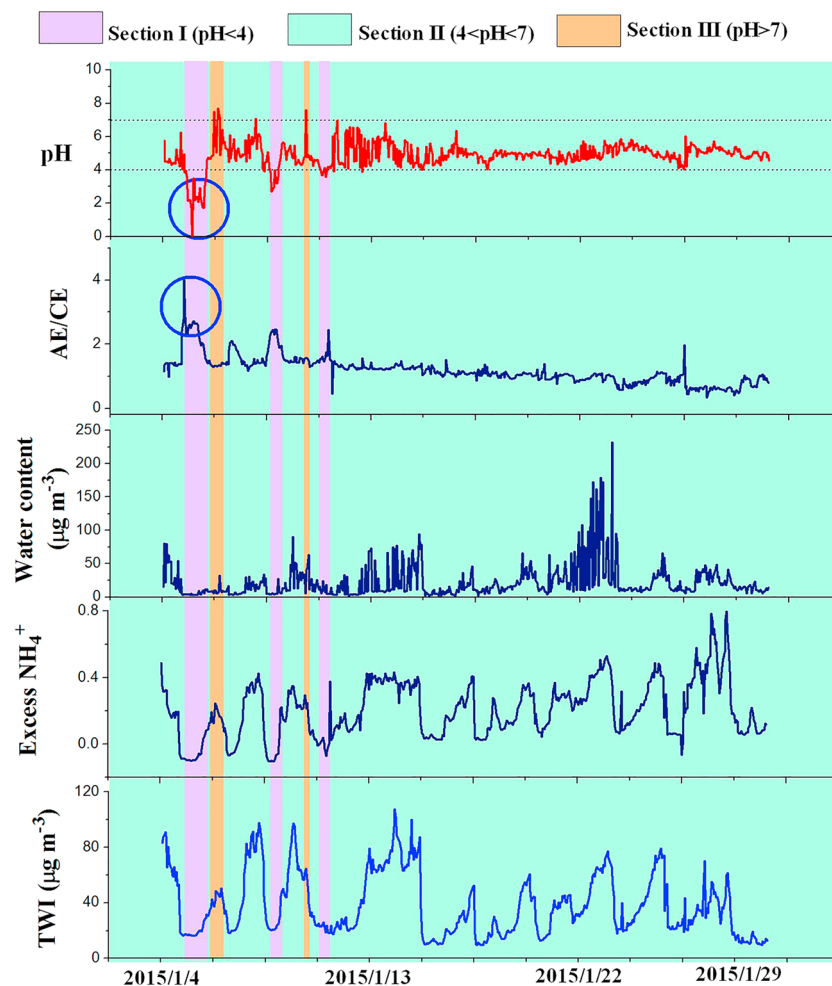


Figure 4. Time series of pH, water content, excess $[\text{NH}_4^+]$, and TWI. Section I, $\text{pH} \leq 4$; Section II, $4 < \text{pH} \leq 7$; Section III, $\text{pH} > 7$. TWI = total water soluble ions ($\text{TWI} < 30 \mu\text{g}/\text{m}^3$: less polluted time period, $\text{TWI} > 30 \mu\text{g}/\text{m}^3$: heavily polluted time period).

$[\text{NH}_4^+] < [\text{NO}_3^-]$) or rich condition (excess $[\text{NH}_4^+] > [\text{NO}_3^-]$; Figure S4a). This leads to a low correlation between pH and secondary nitrate ($R = 0.05$). It was also found that the correlations of all sources in the heavily polluted regime were lower than the correlations in less polluted conditions (Table 1). Lower correlations at higher loadings may suggest that the nonlinearities in the chemistry are magnified. During high-pollution periods, the nonlinear relationship should be increasing due to the nonlinear chemistry. During high-pollution periods, the secondary aerosol was higher than those in the less polluted period. To better explore the role of NH_4^+ and NH_3 (g) in the neutralization of aerosol acidity, the time period was further divided into three sections: aerosol $\text{pH} \leq 4$ (Section I), $4 < \text{pH} \leq 7$ (Section II), and > 7 (Section III; Figure 4). Section I typically occurs during NH_4^+ -poor conditions (excess $[\text{NH}_4^+] < 0$) and when concentrations of nonvolatile cations such as K^+ , Ca^{2+} , Na^+ , and Mg^{2+} were lower. The lack of NH_4^+ and nonvolatile cations to fully neutralize anions leads to high aerosol acidity. In Sections II and III, sufficient NH_4^+ and relatively high nonvolatile cation concentrations were responsible for relatively higher aerosol pH. Further, we also performed regression between pH and source contributions (SPSS 11.2, backward regression) for heavily and less polluted periods, as follows:

1. for heavily polluted periods:

$$\text{pH} = 4.72 + 0.04\text{coal} + 0.04\text{dust} - 0.01\text{SN} - 0.01\text{SS} \quad (R = 0.35) \quad (7)$$

2. for less polluted periods:

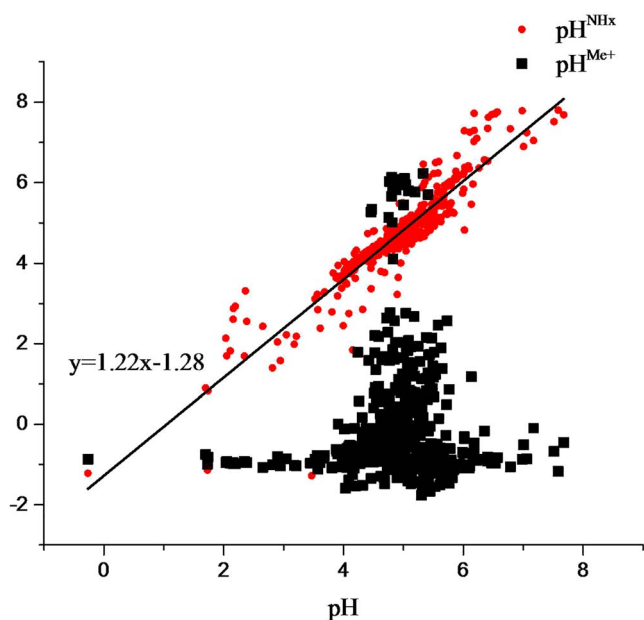


Figure 5. Relationship between pH^{NHx} , pH^{Me^+} , and base pH (pH calculated by ISORROPIA-II using the observed species concentrations). pH^{NHx} : $\text{NH}_3^+(\text{g}) + \text{NH}_4^+$ were kept the same as the observed values (the same as for base pH), but other WS cations were set to zero for ISORROPIA-II; pH^{Me^+} : other WS cations were kept the same as the observed values (the same as for base pH), but $\text{NH}_3(\text{g})$ and NH_4^+ were set to zero for ISORROPIA-II.

$$\text{pH} = 3.69 + 0.05\text{coal} + 0.09\text{dust} - 0.06\text{vehicle} + 0.11\text{SN} - 0.10\text{SS} \quad (R = 0.57) \quad (8)$$

where SN is the secondary nitrate and SS is the secondary sulfate. In the heavily polluted period, the vehicle factor was removed by backward regression due to statistical insignificance ($p > 0.05$), which might be because vehicle contributions are relatively lower (e.g., a smaller fraction) in heavily polluted periods (Figure 2f). Overall, the results from backward regression (detailed information in Table S2) agreed with those of Pearson's R (Table 1): coal and dust are weakly positively correlated with pH while vehicles and secondary sulfate are weakly negatively correlated. The correlation of secondary nitrate with pH is reversed for heavily and less polluted periods. Lower correlations in the more highly polluted periods indicate that the nonlinearities increase. Additionally, the relationships between the activity coefficients of different ions in the aqueous phase as a function of aerosol pH and NH_4^+ are shown in Figure S8 for $\text{RH} > 60\%$. Nonlinear relationships are found, indicating the importance of the nonlinear chemistry and thermodynamics.

In order to further investigate the role of $\text{NH}_4^+/\text{NH}_3(\text{g})$ in the neutralization of aerosol acidity and aerosol growth, we performed ISORROPIA-II simulations to calculate aerosol pH for two hypothetical scenarios: (1) pH^{NHx} , where total ammonia ($\text{NH}_3(\text{g}) + \text{NH}_4^+$), was kept the same but with no other WS-cation inputs to ISORROPIA) and (2) pH^{Me^+} , where nonammonium WS-cation inputs were kept the same but $\text{NH}_3(\text{g})$ and NH_4^+ were removed. Removing the nonammonium cations (pH^{Me^+}) had little impact on pH (Figure 5), while removing the ammonia/ammonium typically led to large reductions in pH (Figure 5). In some

cases, the pH increased with the removal of ammonium due to the change in the solubility of metals and the reduced formation of ammonium nitrate. Likewise, the removal of other cations led to small increases in pH in some cases due to the underestimation (compared with the original pH) of liquid water content (LWC) by the model.

The results suggest that the availability of $\text{NH}_4^+/\text{NH}_3(\text{g})$ is a determining factor in stabilizing pH during heavily polluted periods, while nonvolatile cations contribute less to decreasing aerosol acidity during most periods examined. During the intense haze periods examined here, relatively high pH usually occurs because of the availability of $\text{NH}_4^+/\text{NH}_3(\text{g})$ even at very high sulfate and nitrate levels. During this period, when total ammonia is low, pH and water content are also low, although such occurrences are rare (e.g., right after a period where PM is depleted). It can be seen from Figure 4 that water content increases with concentrations of sulfate, nitrate, and ammonium which all take up substantial water. The increased water content can provide a large aerosol surface and volume, which promotes secondary formation, leading to increased SO_4^{2-} and NO_3^- formation along with increased aerosol partitioning of NH_4^+ (Behera et al., 2013; Y. C. Liu et al., 2017).

3.4. SOR and NOR

We explored secondary formation pathways by analyzing pH, SOR and NOR, TWI, LWC, and other pertinent factors (Figure 6). NOR (average of 0.21) was higher on average than SOR (average of 0.09; Figure 6), suggesting that there is faster nitrate generation than sulfate in winter (or, more precisely, faster oxidation of NO_x versus SO_2), which can also be seen in the concentrations of nitrate and sulfate (Figure 1). The NOR can be also be influenced by the change of partitioning between the particle and gas-phase nitrate, which is affected by temperature and pH (Shi et al., 2019). Weak negative correlations between pH, SOR, and NOR were observed. The correlation of pH and SOR ($R = -0.27$) suggests that a higher SOR lowered pH, as expected. The correlation of pH and NOR ($R = -0.03$) suggests that there is little impact of pH on nitrogen oxidation. Typically NOR was higher than SOR, but occasionally SOR was higher than NOR (e.g., episode A in Figure 6). Episodes with higher sulfate formation rates than nitrate formation rates were associated with

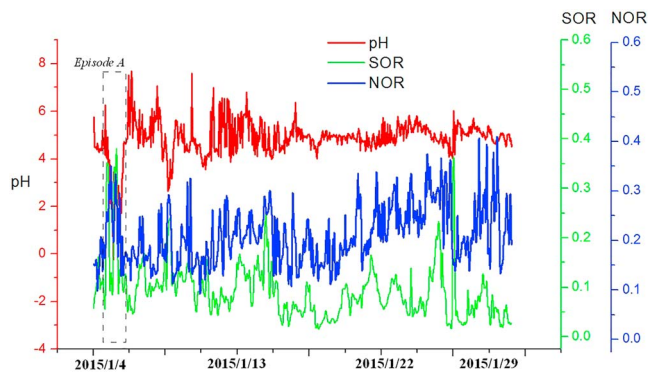


Figure 6. Time series of pH, SOR (sulfur oxidation ratio), and NOR (nitrogen oxidation ratio). For most cases, NOR was higher than SOR. In episode A, SOR was higher than NOR. According to this figure and Figure S9, in this episode, pH, TWI, and water content were low. The results indicate high acidity (pH less than 3), light pollution (TWI less than $30 \mu\text{g}/\text{m}^3$), and low water content (less than $5 \mu\text{g}/\text{m}^3$) in winter were related to a higher sulfate formation rate than nitrate formation rate.

Acknowledgments

This study was supported by the National Key Research and Development Program of China (2016YFC0208500, 2016YFC0208505), National Natural Science Foundation of China (41775149), Special Scientific Research Funds for Environment Protection Commonweal Section (201509020), the Tianjin Research Program of Application Foundation and Advanced Technology (14JQCJNC0810), Tianjin Natural Science Foundation (17JCYBJC23000, 16JQCJNC08700), and the Blue Sky Foundation, Fundamental Research Funds for the Central Universities. This publication was developed under assistance agreement EPA834799 awarded by the U.S. Environmental Protection Agency to the Georgia Institute of Technology and NSF grant 1444745. It has not been formally reviewed by any funding agency and the views expressed in this document are solely those of the authors and do not necessarily reflect those of the agency, nor do those agencies endorse any products or commercial services mentioned in this publication. We also thank G. Pavur for her help in preparing the manuscript. All the data in this study can be found in the supporting information (data file).

0.27) of pH versus SOR in L-SOR might be due to the influence of cation-related sources (coal and dust). In Table S3, coal and dust contribute more (18.8% and 16.3%) during L-SOR than during M- (moderate) and H-SOR (high) conditions. The negative correlation ($R = -0.17$) of LWC versus SOR in H-SOR might be due to faster sulfate generation during daytime, so LWC might be at a lower level when SOR is high. Another reason might be that the LWC is a nonlinear function of the particle components, so LWC should not be expected to have a purely linear relationship with SOR. For LWC versus SOR in L-SOR, a weak correlation was obtained ($R = 0.07$). For TWI versus SOR, the positive correlation ($R = 0.31$) during L-SOR suggests faster sulfate generation along with the TWI increasing for relatively less polluted conditions (mean TWI = $23.1 \mu\text{g}/\text{m}^3$ at L-SOR), while the negative correlation ($R = -0.25$) during H-SOR suggests more pollution (mean TWI = $50.9 \mu\text{g}/\text{m}^3$ at H-SOR) and slower sulfate generation occurred. Similar statistical analyses were also performed for different NOR levels, and the results were in agreement with those for SOR (Table S3).

4. Conclusion

In this work, hourly concentrations of WS ions in $\text{PM}_{2.5}$, along with gaseous pollutants, were observed in Tianjin, China. Sources were estimated with a receptor model, and aerosol pH was estimated by a thermodynamics model. The estimated aerosol pH ranged from -0.3 to 7.7 , with an average value of 4.9 ± 0.8 (mean \pm SD). During less polluted time periods ($\text{TWI} < 30 \mu\text{g}/\text{m}^3$), aerosol pH varied more (from -0.3 to 7.0 with an average of 4.7 ± 0.9) and increased along with the concentration of NH_4^+ or NH_3 (g). During heavily polluted time periods, aerosol pH remained constant at around 5 as measured NH_4^+ (or NH_3 (g)) concentrations increased and became much less responsive to ammonia and ammonium levels. We investigated the relationships among aerosol pH, ammonia, and secondary aerosol formation and found that $\text{NH}_4^+/\text{NH}_3$ (g) plays a determining role in stabilizing pH, while nonvolatile cations contribute less to decreasing aerosol acidity during most of the periods examined. Additionally, after exploring the variability of NOR and SOR, we found that nitrate is produced faster than sulfate in winter, but SOR was much higher than NOR under conditions with high acidity, low pollution, and low water content. The findings of this work show the role of pH on the formation of secondary aerosols under different levels of pollution. Since pH is hard to measure directly, the discussion of pH in this work is based on modeled values. Development of methods and technologies for direct pH measurement are desired for future work.

References

- Al-Dabbous, A. N., & Kumar, P. (2015). Source apportionment of airborne nanoparticles in a Middle Eastern city using positive matrix factorization. *Environmental Science: Processes & Impacts*, 17(4), 802–812. <https://doi.org/10.1039/c5em00027k>
- Amato, F., & Hopke, P. K. (2012). Source apportionment of the ambient $\text{PM}_{2.5}$ across St. Louis using constrained positive matrix factorization. *Atmospheric Environment*, 46, 329–337. <https://doi.org/10.1016/j.atmosenv.2011.09.062>

high acidity (pH less than 3), lower pollution (TWI less than $30 \mu\text{g}/\text{m}^3$), and lower water content (less than $5 \mu\text{g}/\text{m}^3$) in winter (from Figures 6 and S9). Under such situations, ammonia will neutralize acidic sulfate to form $(\text{NH}_4)_2\text{SO}_4$, and the remaining ammonia will react with gaseous nitric acid to form NH_4NO_3 (Huang et al., 2011). During the less polluted period, average concentrations of SO_4^{2-} ($8.9 \mu\text{g}/\text{m}^3$ in episode A) were higher than those of NO_3^- ($6.2 \mu\text{g}/\text{m}^3$ in episode A), while over the entire period, average concentrations of SO_4^{2-} ($11 \mu\text{g}/\text{m}^3$) were lower than those of NO_3^- ($13 \mu\text{g}/\text{m}^3$). Our previous work also showed that when sulfate was dominant, pH could be low (< 4 ; Shi et al., 2017).

We also tested the relationships between SOR and pH, LWC, and TWI under different SOR conditions. As shown in Table S3, during high SOR (H-SOR; $\text{SOR} > 0.10$) levels, the values of Pearson's R for pH versus SOR, LWC versus SOR, and TWI versus SOR were negative (-0.31 , -0.17 , and -0.25), while during low SOR (L-SOR; $\text{SOR} < 0.05$) levels, the values were all positive (0.27 , 0.08 , and 0.34). The negative correlation ($R = -0.31$) of pH versus SOR in H-SOR is easily explained: increased sulfate will make aerosols more acidic. The positive correlation ($R =$

- Amato, F., Pandolfi, M., Escrig, A., Querol, X., Alastuey, A., Pey, J., et al. (2009). Quantifying road dust resuspension in urban environment by Multilinear Engine: A comparison with PMF2. *Atmospheric Environment*, *43*(17), 2770–2780. <https://doi.org/10.1016/j.atmosenv.2009.02.039>
- Behera, S. N., Betha, R., Liu, P., & Balasubramanian, R. (2013). A study of diurnal variations of PM_{2.5} acidity and related chemical species using a new thermodynamic equilibrium mode. *The Science of the Total Environment*, *452–453*, 286–295. <https://doi.org/10.1016/j.scitotenv.2013.02.062>
- Bouwman, A. F., Vuuren, D. P. V., Derwent, R. G., & Posch, M. (2002). A global analysis of acidification and eutrophication of terrestrial ecosystems. *Water, Air, & Soil Pollution*, *141*(1/4), 349–382. <https://doi.org/10.1023/A:1021398008726>
- Cheng, H., Gong, W., Wang, Z., Zhang, F., Wang, X., Lv, X., et al. (2014). Ionic composition of submicron particles (PM_{1.0}) during the long-lasting haze period in January 2013 in Wuhan, central China. *Journal of Environmental Sciences*, *26*(4), 810–817. [https://doi.org/10.1016/S1001-0742\(13\)60503-3](https://doi.org/10.1016/S1001-0742(13)60503-3)
- Cheng, S. H., Yang, L. X., Zhou, X. H., Xue, L. K., Gao, X. M., Zhou, Y., & Wang, W. X. (2011). Size-fractionated water-soluble ions, situ pH and water content in aerosol on hazy days and the influences on visibility impairment in Jinan, China. *Atmospheric Environment*, *45*(27), 4631–4640. <https://doi.org/10.1016/j.atmosenv.2011.05.057>
- Colbeck, I., & Harrison, R. M. (1984). Ozone-secondary aerosol-visibility relationships in North-West England. *Science of the Total Environment*, *34*(1–2), 87–100. [https://doi.org/10.1016/0048-9697\(84\)90043-3](https://doi.org/10.1016/0048-9697(84)90043-3)
- Fang, T., Guo, H. Y., Zeng, L. H., Verma, V., Nenes, A., & Weber, R. J. (2017). Highly acidic ambient particles, soluble metals, and oxidative potential: A link between sulfate and aerosol toxicity. *Environmental Science & Technology*, *51*(5), 2611–2620. <https://doi.org/10.1021/acs.est.6b06151>
- Fountoukis, C., & Nenes, A. (2007). ISORRPOPIA II: A computationally efficient thermodynamic equilibrium model for K⁺-Ca²⁺-Mg²⁺-NH₄⁺-Na⁺-SO₄²⁻-NO₃⁻-Cl⁻-H₂O aerosols. *Atmospheric Chemistry and Physics*, *7*(17), 4639–4659. <https://doi.org/10.5194/acp-7-4639-2007>
- Gao, J. J., Tian, H. Z., Cheng, K., Lu, L., Zheng, M., Wang, S. X., et al. (2015). The variation of chemical characteristics of PM_{2.5} and PM₁₀ and formation causes during two haze pollution events in urban Beijing, China. *Atmospheric Environment*, *107*, 1–8. <https://doi.org/10.1016/j.atmosenv.2015.02.022>
- Guo, H., Sullivan, A. P., Campuzano-Jost, P., Schroder, J. C., Lopez-Hilfiker, F. D., Dibb, J. E., et al. (2016). Fine particle pH and the partitioning of nitric acid during winter in the northeastern United States. *Journal of Geophysical Research: Atmospheres*, *121*, 10,355–10,376. <https://doi.org/10.1002/2016JD025311>
- Guo, H., Xu, L., Bougiatioti, A., Cerully, K. M., Capps, S. L., Hite, J. R. Jr., et al. (2015). Fine-particle water and pH in the southeastern United States. *Atmospheric Chemistry and Physics*, *15*(9), 5211–5228. <https://doi.org/10.5194/acp-15-5211-2015>
- Guo, H. Y., Weber, R. J., & Nenes, A. (2017). High levels of ammonia do not raise fine particle pH sufficiently to yield nitrogen oxide-dominated sulfate production. *Scientific Reports*, *7*(1), 12109. <https://doi.org/10.1038/s41598-017-11704-0>
- Habre, R., Coull, B., & Koutrakis, P. (2011). Impact of source collinearity in simulated PM_{2.5} data on the PMF receptor model solution. *Atmospheric Environment*, *45*(38), 6938–6946. <https://doi.org/10.1016/j.atmosenv.2011.09.034>
- He, H., Zhao, Q. Q., Ma, Y., & Yang, F. M. (2012). Spatial and seasonal variability of PM_{2.5} acidity at two Chinese megacities: Insights into the formation of secondary inorganic aerosols. *Atmospheric Chemistry and Physics*, *12*(3), 1377–1395. <https://doi.org/10.5194/acp-12-1377-2012>
- Hennigan, C. J., Izumi, J., Sullivan, A. P., Weber, R. J., & Nenes, A. (2015). A critical evaluation of proxy methods used to estimate the acidity of atmospheric particles. *Atmospheric Chemistry and Physics*, *15*(5), 2775–2790. <https://doi.org/10.5194/acp-15-2775-2015>
- Hu, G. Y., Zhang, Y. M., Sun, J. Y., Zhang, L. M., Shen, X. J., Lin, W. L., & Yang, Y. (2014). Variability, formation and acidity of water-soluble ions in PM_{2.5} in Beijing based on the semi-continuous observations. *Atmospheric Research*, *145–146*, 1–11. <https://doi.org/10.1016/j.atmosres.2014.03.014>
- Huang, X., Qiu, R., Chan, C. K., & Kant, P. R. (2011). Evidence of high PM_{2.5} strong acidity in ammonia-rich atmosphere of Guangzhou, China: Transition in pathways of ambient ammonia to form aerosol ammonium at [NH₄⁺]/[SO₄²⁻] = 1.5. *Atmospheric Research*, *99*(3–4), 488–495. <https://doi.org/10.1016/j.atmosres.2010.11.021>
- Huo, M. Q., Sun, Q., Bai, Y. H., Li, J. L., Xie, P., Liu, Z. R., & Wang, X. (2012). Influence of airborne particles on the acidity of rainwater during wash-out process. *Atmospheric Environment*, *59*, 192–201. <https://doi.org/10.1016/j.atmosenv.2012.05.035>
- Jang, M., Czoschke, N. M., Lee, S., & Kamens, R. M. (2002). Heterogeneous atmospheric aerosol production by acid-catalyzed particle-phase reactions. *Science*, *298*(5594), 814–817. <https://doi.org/10.1126/science.1075798>
- Jia, S., Wang, X., Zhang, Q., Sarkar, S., Wu, L., Huang, M., et al. (2018). Technical note: Comparison and interconversion of pH based on different standard states for aerosol acidity characterization. *Atmospheric Chemistry and Physics*, *18*(15), 11125–11133. <https://doi.org/10.5194/acp-18-11125-2018>
- Kaneyasu, N., Yoshikado, H., Mizuno, T., Sakamoto, K., & Soufuku, M. (1999). Chemical forms and sources of extremely high nitrate and chloride in winter aerosol pollution in the Kanto Plain of Japan. *Atmospheric Environment*, *33*(11), 1745–1756. [https://doi.org/10.1016/S1352-2310\(98\)00396-3](https://doi.org/10.1016/S1352-2310(98)00396-3)
- Lawal, A. S., Guan, X., Liu, C., Henneman, L. R., Vasilakos, P., Bhogineni, V., et al. (2018). Linked response of aerosol acidity and ammonia to SO₂ and NO_x emissions reductions in the United States. *Environmental Science & Technology*, *52*(17), 9861–9873. <https://doi.org/10.1021/acs.est.8b00711>
- Li, H. Y., Zhang, Q., Zheng, B., Chen, C. R., Wu, N. N., Guo, H. Y., et al. (2018). Nitrate-driven urban haze pollution during summertime over the North China Plain. *Atmospheric Chemistry and Physics*, *18*(8), 5293–5306. <https://doi.org/10.5194/acp-18-5293-2018>
- Li, L. J., Hoffmann, M. R., & Colussi, A. J. (2018). Role of nitrogen dioxide in the production of sulfate during Chinese haze-aerosol episodes. *Environmental Science & Technology*, *52*(5), 2686–2693. <https://doi.org/10.1021/acs.est.7b05222>
- Liu, S., Hu, M., Slanina, S., He, L. Y., Niu, Y. W., Bruegemann, E., et al. (2008). Size distribution and source analysis of ionic compositions of aerosols in polluted periods at Xinken in Pearl River Delta (PRD) of China. *Atmospheric Environment*, *42*(25), 6284–6295. <https://doi.org/10.1016/j.atmosenv.2007.12.035>
- Liu, Y. C., Wu, Z. J., Wang, Y., Xiao, Y., Gu, F. T., Zheng, J., et al. (2017). Submicrometer particles are in the liquid state during heavy haze episodes in the urban atmospheric of Beijing, China. *Environmental Science & Technology Letters*, *4*(10), 427–432. <https://doi.org/10.1021/acs.estlett.7b00352>
- Manousakas, M., Diapouli, E., Papaefthymiou, H., Migliori, A., Karydas, A. G., Padilla-Alvarez, R., et al. (2015). Source apportionment by PMF on elemental concentrations obtained by PIXE analysis of PM₁₀ samples collected at the vicinity of lignite power plants and mines in Megalopolis, Greece. *Nuclear Instruments and Methods in Physics Research Section B*, *349*, 114–124. <https://doi.org/10.1016/j.nimb.2015.02.037>

- McMurry, P. H., Takano, H., & Anderson, G. R. (1983). Study of the ammonia (gas)-sulfuric acid (aerosol) reaction rate. *Environmental Science & Technology*, *17*(6), 347–352. <https://doi.org/10.1021/es00112a008>
- Meskhidze, N., Chameides, W. L., Nenes, A., & Chen, G. (2003). Iron mobilization in mineral dust: Can anthropogenic SO₂ emissions affect ocean productivity? *Geophysical Research Letters*, *30*(21), 2085. <https://doi.org/10.1029/2003GL018035>
- Murphy, J. G., Gregoire, P. K., Tevlin, A. G., Wentworth, G. R., Ellis, R. A., Markovic, M. Z., & VandenBoer, T. C. (2017). Observational constraints on particle acidity using measurements and modelling of particles and gases. *Faraday Discussions*, *200*, 379–395. <https://doi.org/10.1039/c7fd00086c>
- Ohta, S., & Okita, T. A. (1990). A chemical characterization of atmospheric aerosol in Sapporo. *Atmospheric Environment*, *24*(4), 815–822. [https://doi.org/10.1016/0960-1686\(90\)90282-R](https://doi.org/10.1016/0960-1686(90)90282-R)
- Paatero, P. (2007). *End user's guide to multilinear engine applications*.
- Paatero, P., & Tapper, U. (1994). Positive matrix factorization: A non-negative factor model with optimal utilization of error estimates of data values. *Environmetrics*, *5*(2), 111–126. <https://doi.org/10.1002/env.3170050203>
- Pandis, S. N., & Seinfeld, J. H. (1989). Sensitivity analysis of a chemical mechanism for aqueous-phase atmospheric chemistry. *Journal of Geophysical Research*, *94*(D1), 1105–1126. <https://doi.org/10.1029/JD094iD01p01105>
- Parworth, C., Fast, J., Mei, F., Shippert, T., Sivaraman, C., Tilp, A., et al. (2015). Long-term measurements of submicrometer aerosol chemistry at the Southern Great Plains (SGP) using an Aerosol Chemical Speciation Monitor (ACSM). *Atmospheric Environment*, *106*, 43–55. <https://doi.org/10.1016/j.atmosenv.2015.01.060>
- Pattatys, A. K., Businger, S., & Howell, S. G. (2018). Review of sulfur dioxide to sulfate aerosol chemistry at Kilauea Volcano, Hawai'i. *Atmospheric Environment*, *185*, 262–271. <https://doi.org/10.1016/j.atmosenv.2018.04.055>
- Putaud, J. P., Dingenen, R. V., Dell'Acqua, A., & Sandro, F. (2004). Size-segregated aerosol mass closure and chemical composition in Monte Cimone (I) during MINATROC. *Atmospheric Chemistry and Physics*, *3*(4), 4097–4127. <https://doi.org/10.5194/acpd-3-4097-2003>
- Ren, L., Wang, W., Wang, Q., Yang, X. Y., & Tang, D. (2011). Comparison and trend study on acidity and acidic buffering capacity of particulate matter in China. *Atmospheric Environment*, *45*(39), 7503–7519. <https://doi.org/10.1016/j.atmosenv.2010.08.055>
- Shao, P. Y., Tian, H. Z., Sun, Y. J., Liu, H. J., Wu, B. B., Liu, S. H., et al. (2018). Characterizing remarkable changes of severe haze events and chemical compositions in multi-size airborne particles (PM₁, PM_{2.5} and PM₁₀) from January 2013 to 2016–2017 winter in Beijing, China. *Atmospheric Environment*, *189*, 133–144. <https://doi.org/10.1016/j.atmosenv.2018.06.038>
- Shen, Z., Cao, J., Arimoto, R., Han, Z., Zhang, R., Han, Y., et al. (2009). Ionic composition of TSP and PM_{2.5} during dust storms and air pollution episodes at Xi'an, China. *Atmospheric Environment*, *43*(18), 2911–2918. <https://doi.org/10.1016/j.atmosenv.2009.03.005>
- Shen, Z. X., Cao, J. J., Liu, S. X., Zhu, C. S., Wang, X., Zhang, T., et al. (2011). Chemical composition of PM₁₀ and PM_{2.5} collected at ground level and 100 meters during a strong winter-time pollution episode in Xi'an, China. *Journal of the Air & Waste Management Association*, *61*(11), 1150–1159. <https://doi.org/10.1080/10473289.2011.608619>
- Shi, G. L., Xu, J., Peng, X., Xiao, Z. M., Chen, K., Tian, Y. Z., et al. (2017). pH of aerosols in a polluted atmosphere: Source contributions to highly acidic aerosol. *Environmental Science & Technology*, *51*(8), 4289–4296. <https://doi.org/10.1021/acs.est.6b05736>
- Shi, X. R., Nenes, A., Xiao, Z. M., Song, S. J., Yu, H. F., Shi, G. L., et al. (2019). High-resolution datasets unravel the effects of sources and meteorological conditions on nitrate and its gas-particle partitioning. *Environmental Science & Technology*, *53*(6), 3048–3057. <https://doi.org/10.1021/acs.est.8b06524>
- Silvern, R. F., Jacob, D. J., Kim, P. S., Marais, E. A., Turner, J. R., Campuzano-Jost, P., & Jimenez, J. L. (2017). Inconsistency of ammonium-sulfate aerosol ratios with thermodynamic models in the eastern US: A possible role of organic aerosol. *Atmospheric Chemistry and Physics*, *17*(8), 5107–5118. <https://doi.org/10.5194/acp-17-5107-2017>
- Song, S. J., Gao, M., Xu, W. Q., Shao, J. Y., Shi, G. L., Wang, S. X., et al. (2018). Fine-particle pH for Beijing winter haze as inferred from different thermodynamic equilibrium models. *Atmospheric Chemistry and Physics*, *18*(10), 7423–7438. <https://doi.org/10.5194/acp-18-7423-2018>
- Song, S. J., Gao, M., Xu, W. Q., Sun, Y. L., Worsnop, D. R., Jayne, J. T., et al. (2019). Possible heterogeneous chemistry of hydroxymethanesulfonate (HMS) in northern China winter haze. *Atmospheric Chemistry and Physics*, *19*(2), 1357–1371. <https://doi.org/10.5194/acp-19-1357-2019>
- Sun, J., Zhang, Q., Canagaratna, M. R., Zhang, Y. M., Ng, N. L., Sun, Y., et al. (2010). Highly time- and size-resolved characterization of submicron aerosol particles in Beijing using an Aerodyne Aerosol Mass Spectrometer. *Atmospheric Environment*, *44*(1), 131–140. <https://doi.org/10.1016/j.atmosenv.2009.03.020>
- Surratt, J. D., Chana, A. W. H., Eddingsaas, N. C., Chan, M. N., Loza, C. L., & Kwan, et al. (2010). Reactive intermediates revealed in secondary organic aerosol formation from isoprene. *Proceedings of the National Academy of Sciences of the United States of America*, *107*(15), 6640–6645. <https://doi.org/10.1073/pnas.0911114107>
- Tang, J., Xu, X. B., Ba, J., & Wang, S. F. (2010). Trends of the precipitation acidity over China during 1992–2006. *Chinese Science Bulletin*, *55*(17), 1800–1807. <https://doi.org/10.1007/s11434-009-3618-1>
- Wang, W., Liu, H. J., Yue, X., Li, H., Chen, J. H., Ren, L. H., et al. (2006). Study on acidity and acidic buffering capacity of particulate matter over Chinese eastern coastal areas in spring. *Journal of Geophysical Research*, *111*, D18207. <https://doi.org/10.1029/2005JD006753>
- Weber, R. J., Guo, H., Russell, A. G., & Nenes, A. (2016). High aerosol acidity despite declining atmospheric sulfate concentrations over the past 15 years. *Nature Geoscience*, *9*(4), 282–285. <https://doi.org/10.1038/ngeo2665>
- Wu, W. S., & Wang, T. (2007). On the performance of a semi-continuous PM_{2.5} sulphate and nitrate instrument under high loadings of particulate and sulphur dioxide. *Atmospheric Environment*, *41*(26), 5442–5451. <https://doi.org/10.1016/j.atmosenv.2007.02.025>
- Xu, L. L., Duan, F. K., He, K. B., Ma, Y. L., Zhu, L. D., Zheng, Y. X., et al. (2017). Characteristics of the secondary water-soluble ions in a typical autumn haze in Beijing. *Environmental Pollution*, *227*, 296–305. <https://doi.org/10.1016/j.envpol.2017.04.076>
- Yang, F., Tan, J., Zhao, Q., Du, Z., He, K., Ma, Y., et al. (2011). Characteristics of PM_{2.5} speciation in representative megacities and across China. *Atmospheric Chemistry and Physics*, *11*(11), 5207–5219. <https://doi.org/10.5194/acp-11-5207-2011>
- Yu, Q., Chen, J., Qin, W. H., Cheng, S. M., Zhang, Y. P., Ahmad, M., & Ouyang, W. (2019). Characteristics and secondary formation of water-soluble organic acids in PM₁, PM_{2.5} and PM₁₀ in Beijing during haze episodes. *Science of the Total Environment*, *669*, 175–184. <https://doi.org/10.1016/j.scitotenv.2019.03.131>
- Yue, D. L., Hu, M., Wu, Z. J., & Liu, S. C. (2009). Characteristics of aerosol size distributions and new particle formation in the summer in Beijing. *Journal of Geophysical Research*, *114*, D00G12. <https://doi.org/10.1029/2008JD010894>
- Zhang, Q., Shen, Z., Cao, J., Zhang, R., Zhang, L., Huang, R. J., et al. (2015). Variations in PM_{2.5}, TSP, BC, and trace gases (NO₂, SO₂, and O₃) between haze and non-haze episodes in winter over Xi'an, China. *Atmospheric Environment*, *112*, 64–71. <https://doi.org/10.1016/j.atmosenv.2015.04.033>

- Zhang, X. Y., Wang, Y. Q., Niu, T., Zhang, X. C., Gong, S. L., Zhang, Y. M., & Sun, J. Y. (2012). Atmospheric aerosol compositions in China: Spatial/temporal variability, chemical signature, regional haze distribution and comparisons with global aerosols. *Atmospheric Chemistry and Physics*, *12*(2), 779–799. <https://doi.org/10.5194/acp-12-779-2012>
- Ziemba, L. D., Fischer, E., Griffin, R. J., & Talbot, R. W. (2007). Aerosol acidity in rural New England: Temporal trends and source region analysis. *Journal of Geophysical Research*, *112*, D10S22. <https://doi.org/10.1029/2006JD007605>

References From the Supporting Information

- Anlauf, K., Li, S. M., Leaith, R., Brook, J., Hayden, K., Toom-Sauntry, D., & Wiebe, A. (2006). Ionic composition and size characteristics of particles in the Lower Fraser Valley: Pacific 2001 field study. *Atmospheric Environment*, *40*(15), 2662–2675. <https://doi.org/10.1016/j.atmosenv.2005.12.027>
- Charron, A., Degrendele, C., & Laongsri, B. (2013). Receptor modelling of secondary and carbonaceous particulate matter at a southern UK site. *Atmospheric Chemistry and Physics*, *13*(4), 1879–1894. <https://doi.org/10.5194/acp-13-1879-2013>
- Eddingsaas, N. C., VanderVelde, D. G., & Wennberg, P. O. (2010). Kinetics and products of the acid-catalyzed ring-opening of atmospherically relevant butyl epoxy alcohols. *Journal of Physical Chemistry A*, *114*(31), 8106–8113. <https://doi.org/10.1021/jp103907c>
- Etyemezian, V., Tesfaye, M., Yimer, A., Chow, J. C., Mesfin, D., Nega, T., et al. (2005). Results from a pilot-scale air quality study in Addis Ababa, Ethiopia. *Atmospheric Environment*, *39*(40), 7849–7860. <https://doi.org/10.1016/j.atmosenv.2005.08.033>
- Gao, J., Peng, X., Chen, G., Xu, J., Shi, G. L., Zhang, Y. C., & Feng, Y. C. (2016). Insights into the chemical characterization and sources of PM_{2.5} in Beijing at a 1-h time resolution. *Science of the Total Environment*, *542*(Pt A), 162–171. <https://doi.org/10.1016/j.scitotenv.2015.10.082>
- Gieré, R., Smith, K., & Blackford, M. (2006). Chemical composition of fuels and emissions from a coal + tire combustion experiment in a power station. *Fuel*, *85*(16), 2278–2285. <https://doi.org/10.1016/j.fuel.2005.11.024>
- Hien, P. D., Hangartner, M., Fabian, S., & Tan, P. M. (2014). Concentrations of NO₂, SO₂, and benzene across Hanoi measured by passive diffusion samplers. *Atmospheric Environment*, *88*, 66–73. <https://doi.org/10.1016/j.atmosenv.2014.01.036>
- Hopke, P. K. (1985). *Receptor modeling in environmental chemistry*. New York: John Wiley & Sons.
- Kwok, R. H. F., Napelenok, S. L., & Baker, K. R. (2013). Implementation and evaluation of PM_{2.5} source contribution analysis in a photochemical model. *Atmospheric Environment*, *80*, 398–407. <https://doi.org/10.1016/j.atmosenv.2013.08.017>
- Liggio, J., Li, S. M., & McLaren, R. (2005). Heterogeneous reactions of glyoxal on particulate matter: Identification of acetals and sulfate esters. *Environmental Science & Technology*, *39*(6), 1532–1541. <https://doi.org/10.1021/es048375y>
- Mooibroek, D., Schaap, M., Weijers, E. P., & Hoogerbrugge, R. (2011). Source apportionment and spatial variability of PM_{2.5} using measurements at five sites in the Netherlands. *Atmospheric Environment*, *45*(25), 4180–4191. <https://doi.org/10.1016/j.atmosenv.2011.05.017>
- Nyambura, M. G., Mugeru, G. W., Felicia, P. L., & Gathura, N. P. (2011). Carbonation of brine impacted fractionated coal fly ash: Implications for CO₂ sequestration. *Journal of Environmental Management*, *92*(3), 655–664. <https://doi.org/10.1016/j.jenvman.2010.10.008>
- Pakkanen, T. A. (1996). Study of formation of coarse particle nitrate aerosol. *Atmospheric Environment*, *30*(14), 2475–2482. [https://doi.org/10.1016/1352-2310\(95\)00492-0](https://doi.org/10.1016/1352-2310(95)00492-0)
- Pant, P., & Harrison, R. M. (2012). Critical review of receptor modelling for particulate matter: A case study of India. *Atmospheric Environment*, *49*, 1–12. <https://doi.org/10.1016/j.atmosenv.2011.11.060>
- Sandford, R. C., Exenberger, A., & Worsfold, P. J. (2007). Nitrogen cycling in natural waters using in situ, reagentless UV spectrophotometry with simultaneous determination of nitrate and nitrite. *Environmental Science & Technology*, *41*(24), 8420–8425. <https://doi.org/10.1021/es071447b>
- Song, Y., Xie, S. D., Zhang, Y. H., Zeng, L. M., Salmon, L. G., & Zheng, M. (2006). Source apportionment of PM_{2.5} in Beijing using principal component analysis/absolute principal component scores and UNMIX. *Science of the Total Environment*, *372*(1), 278–286. <https://doi.org/10.1016/j.scitotenv.2006.08.041>
- Tian, Y. Z., Shi, G. L., Han, S. Q., Zhang, Y. F., Feng, Y. C., Liu, G. R., et al. (2013). Vertical characteristics of levels and potential sources of water-soluble ions in PM₁₀ in a Chinese megacity. *Science of the Total Environment*, *447*(49), 1–9. <https://doi.org/10.1016/j.scitotenv.2012.12.071>
- Tianjin Statistical Yearbook (2015). <http://www.stats-tj.gov.cn/Item/26545.aspx>
- Tsai, J. H., Chang, L. P., & Chiang, H. L. (2014). Airborne pollutant characteristics in an urban, industrial and agricultural complex metroplex with high emission loading and ammonia concentration. *Science of the Total Environment*, *494–495*, 74–83. <https://doi.org/10.1016/j.scitotenv.2014.06.120>
- Waked, A., Favez, O., Alleman, L. Y., Piot, C., Petit, J. E., Delaunay, T., et al. (2013). Source apportionment of PM₁₀ in a North-Western Europe regional urban background site (Lens, France) using positive matrix factorization and including primary biogenic emissions. *Atmospheric Chemistry and Physics*, *14*(7), 3325–3346. <https://doi.org/10.5194/acp-14-3325-2014>
- Wang, Y., Zhuang, G., Sun, Y., & An, Z. (2006). The variation of characteristics and formation mechanisms of aerosols in dust, haze, and clear days in Beijing. *Atmospheric Environment*, *40*(34), 6579–6591. <https://doi.org/10.1016/j.atmosenv.2006.05.066>
- Wang, Y., Zhuang, G. S., Zhang, X. Y., Huang, K., Xu, C., Tang, A., et al. (2006). The ion chemistry, seasonal cycle, and sources of PM_{2.5} and TSP aerosol in Shanghai. *Atmospheric Environment*, *40*(16), 2935–2952. <https://doi.org/10.1016/j.atmosenv.2005.12.051>
- Wei, Z., Wang, L. T., Chen, M. Z., & Zheng, Y. (2014). The 2013 severe haze over the Southern Hebei, China: PM_{2.5} composition and source apportionment. *Atmospheric Pollution Research*, *5*(4), 759–768. <https://doi.org/10.5094/APR.2014.085>
- Yao, L., Yang, L. X., Yuan, Q., Yan, C., Dong, C., Meng, C. Q., et al. (2016). Sources apportionment of PM_{2.5} in a background site in the North China Plain. *Science of the Total Environment*, *541*, 590–598. <https://doi.org/10.1016/j.scitotenv.2015.09.123>
- Zhang, N., Han, B., He, F., Xu, J., Niu, C., Zhou, J., et al. (2015). Characterization, health risk of heavy metals, and source apportionment of atmospheric PM_{2.5} to children in summer and winter: An exposure panel study in Tianjin, China. *Air Quality, Atmosphere and Health*, *8*(4), 347–357. <https://doi.org/10.1007/s11869-014-0289-0>
- Zhang, R., Jing, J., Tao, J., & Hsu, S. C. (2013). Chemical characterization and source apportionment of PM_{2.5} in Beijing: Seasonal perspective. *Atmospheric Chemistry and Physics*, *13*(14), 7053–7074. <https://doi.org/10.5194/acp-13-7053-2013>
- Zhang, T., Cao, J. J., Tie, X. X., Shen, Z. X., Liu, S. X., Ding, H., et al. (2011). Water-soluble ions in atmospheric aerosols measured in Xi'an, China: Seasonal variations and sources. *Atmospheric Research*, *102*(1–2), 110–119. <https://doi.org/10.1016/j.atmosres.2011.06.014>
- Zhuang, H., Chan, C. K., Fang, M., & Wexler, A. S. (1999). Formation of nitrate and non-sea-salt sulfate on coarse particles. *Atmospheric Environment*, *33*(26), 4223–4233. [https://doi.org/10.1016/S1352-2310\(99\)00186-7](https://doi.org/10.1016/S1352-2310(99)00186-7)